Surface-based multi-scale network analysis of visuo-motor brain activity: a human 3T fMRI study

Roland E. Berkemeier[1,2,3,★], Oliver Speck[4] & Tonio Ball[1,3,5,★]

[1] Excellence Cluster 'BrainLinks-BrainTools' | [2] Institute of Biology III, Faculty of Biology | [3] Intracranial EEG Lab | ★ Albert-Ludwigs-University, Freiburg, Germany | [4] Department of Biomedical Resonance, Faculty of Natural Sciences, Otto-von-Guericke University, Magdeburg, Germany | [5] Epilepsy Center, University Medical Center, Albert-Ludwigs-University, Freiburg Germany

#1608 OHBM 2015 Annual Meeting June 14-18, 2015, Hawaii Convention Center

Introduction

An array of imaging techniques has been employed to understand the network organization of the human brain, including functional magnetic resonance imaging (fMRI). While several fMRI techniques exist, it is most common to measure the blood oxygen level dependent (BOLD) contrast signal to probe variations of brain activity. When analyzing BOLD signals, a typical processing step is to spatially smooth the data with a Gaussian filter in order to improve the signal-to-noise ratio. In standard fMRI methodology, single volumetric kernels are employed to this aim. However, this approach seems ill suited to the sheet-like nature of the cortex on one hand [Andrade et al., 2001; Ball et al., 2012; Jo et al., 2007, 2008], and its inherently hierarchical spatial organization on the other, as functional units such as local– to brain-wide neuronal networks exist over a broad range of spatial scales.

Methods

- 3-Tesla fMRI study: 5 subjects, visually cued finger movement task
- wide range of brain areas: sensorimotor and prefrontal cortices
- novel **surface-based**, **multi-scale** approach (Fig. 1)
- **structure-enhanced EPI** scans used for re-alignment, co-registration of functional images to avoid T_1/T_2^* cross-modality inaccuracies
- cortical surface segmentation with **geodetic distance estimation**

BOLD response patterns were detected using multiple filter kernels (2-20 mm Full-Width at Half Maximum, FWHM). Functionally correlated, statistically significant (sign-tested, FDR-corrected, q<0.01) Z-score peaks were then evaluated in a network analysis. Finally, we estimated the distances between regional nodes and evaluated their relationship with the filter sizes best suited to detect functional correlations.

Results

A large part of functional processes took place on large (cm) spatial scales previously undetected with established single-filter processing methods. Z-score peaks detected with **large filter kernels** (11-20 mm FWHM) generally showed **more robust functional correlations** than those detected at smaller observation scales (0-10 mm FWHM), although some degree of **scale preference** could be seen in the connection patterns **between specific regions** (Fig. 2). We then discovered functional sub-networks operating at different spatial scales, including a sub-network arranged around the ipsilateral motor cortex with spatially more specific connectivity than those of contralateral areas. This analysis further showed that **large filter kernels** were well suited to detect functional connections **over both short and long distances**, whereas **small filters** only fitted on optimally in such cases where **long-distance connections between contra– and ipsilateral sensorimotor cortices** were involved (Fig. 3).

Conclusion

- Analyses based on the Matched Filter Theorem [Rosenfeld and Kak, 1982] and Gaussian scale-space model [Lindeberg, 1993], can be combined with a surface-based analysis approach.
- Different networks co-exist on different preferred scales.
- Inter-hemispheric connections are spatially more precise, whereas intra-hemispheric connections are more diffuse.
- Scale-space network analysis of brain activity may be used to probe the "network-of-networks" functional organization of cortical activity.

References

Andrade A, Kherif F, Mangin JF, Worsley KJ, Paradis AL, Simon O, Dehaene S, Le Bihan D, Poline JB (2001): Detection of fMRI activation using cortical surface mapping. Hum Brain Mapp 12:79–93.
Ball T, Breckel TPK, Mutschler I, Aertsen A, Schulze-Bonhage A, Hennig J, Speck O (2012): Variability of fMRI-response patterns at different spatial observation scales. Hum Brain Mapp 33:1155–1171.
Jo HJ, Lee J-M, Kim J-H, Choi C-H, Gu B-M, Kang D-H, Ku J, Kwon JS, Kim SI (2008): Artificial shifting of fMRI activation localized by volume- and surface-based analyses. NeuroImage 40:1077–1089.
Jo HJ, Lee J-M, Kim J-H, Shin Y-W, Kim I-Y, Kwon JS, Kim SI (2007): Spatial accuracy of fMRI activation influenced by volume- and surface-based spatial smoothing techniques. NeuroImage 34:550–564.
Lindeberg T (1993): Scale-Space Theory in Computer Vision. Springer.
Rosenfeld A, Kak AC (1982): Digital picture processing. Academic Press.

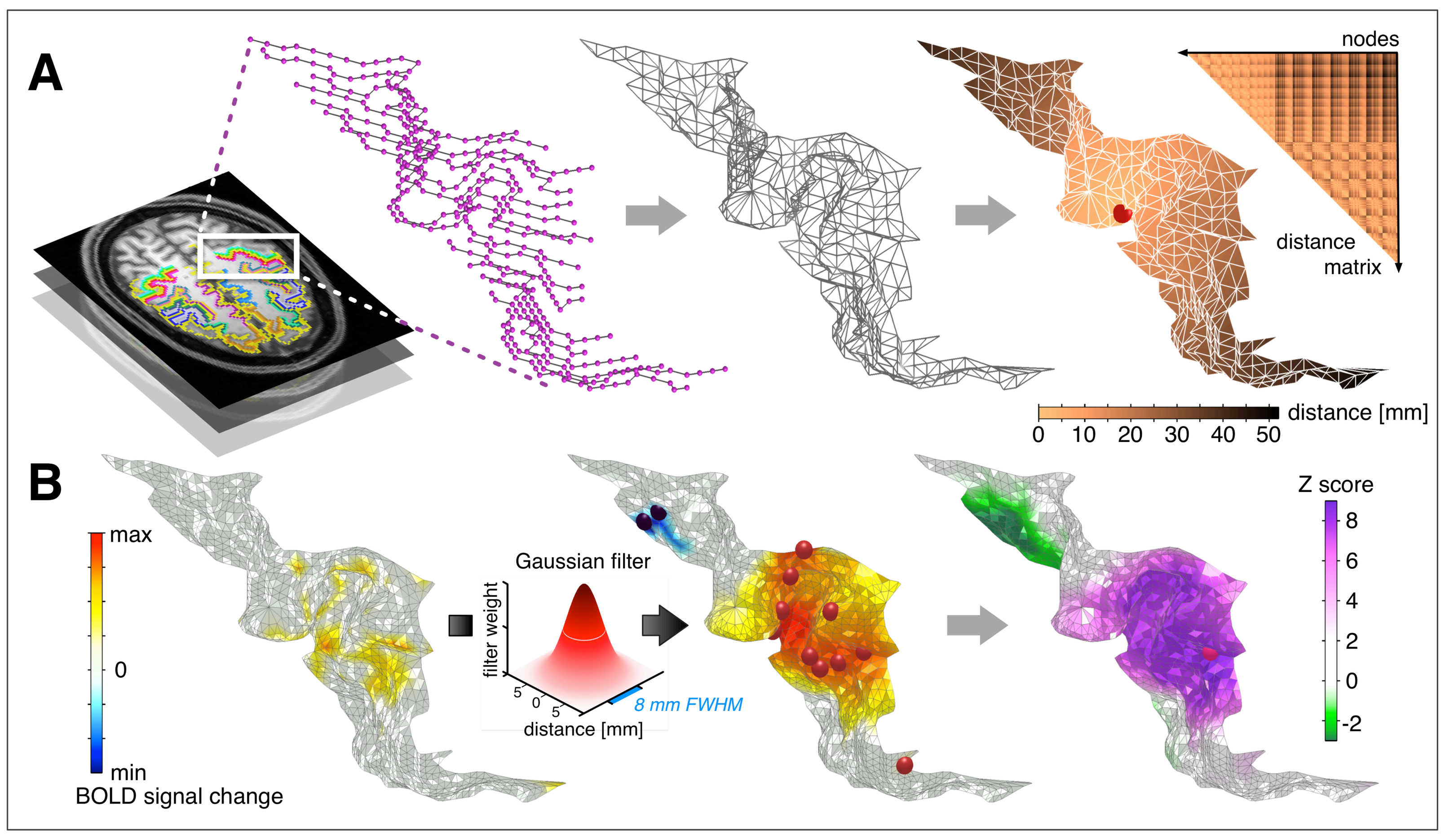

Figure 1: Cortical surface segmentation. A) For every recorded MRI slice, 2 adjacent layers of grey matter (2×1.5 mm width) are marked using in-house software and triangulated in MathWorks MATLAB. Inter-voxel distances are calculated with the Fast Marching algorithm (Gabriel Peyré, CNRS, France). **B)** Gaussian filter kernels (2-20 mm FWHM) are applied to the raw BOLD signal to reveal activity (8 mm FWHM example shown). Statistical analysis (FDR-correction, q<0.01) and peak detection are performed to show hemodynamic activity maps.

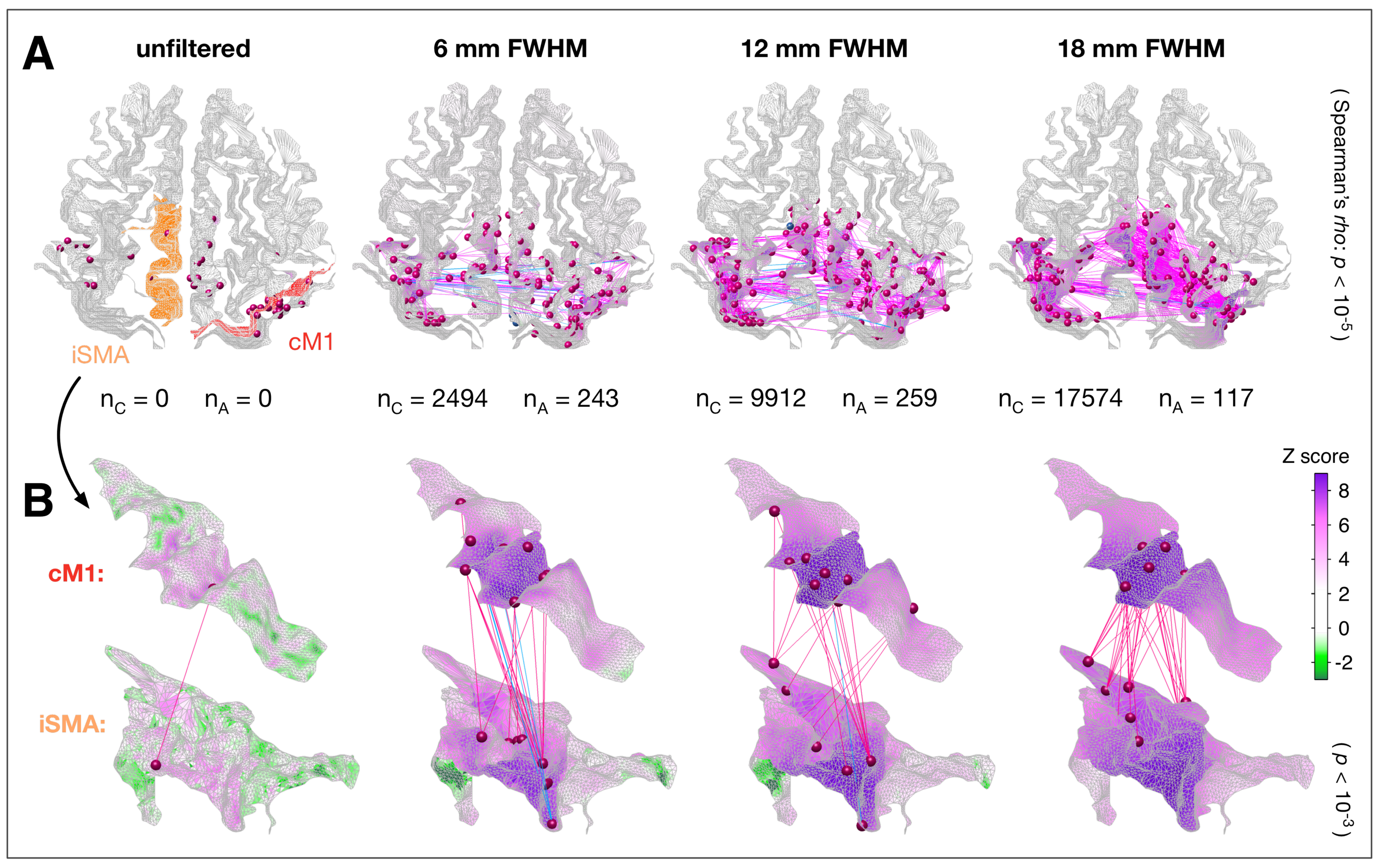

Figure 2: Scale-dependent functional variability of BOLD activity maps. A) Typical un-directed connectivity maps based on previously detected peaks are shown at various observation scales for one subject, 1.5 s post-stimulus. Purple and blue markers show the location of positive and negative activity peaks, respectively. Magenta and blue lines represent significant peak correlation (Spearman's rho , $p < 10^{-5}$), n_C and n_A are the number of correlated and anti-correlated connections, respectively. **B)** shows the detailed connectivity patterns between superficial contralateral primary motor (cM1) and ipsilateral supplementary motor (iSMA) areas. The same color conventions as above apply (significance here is $p < 10^{-3}$).

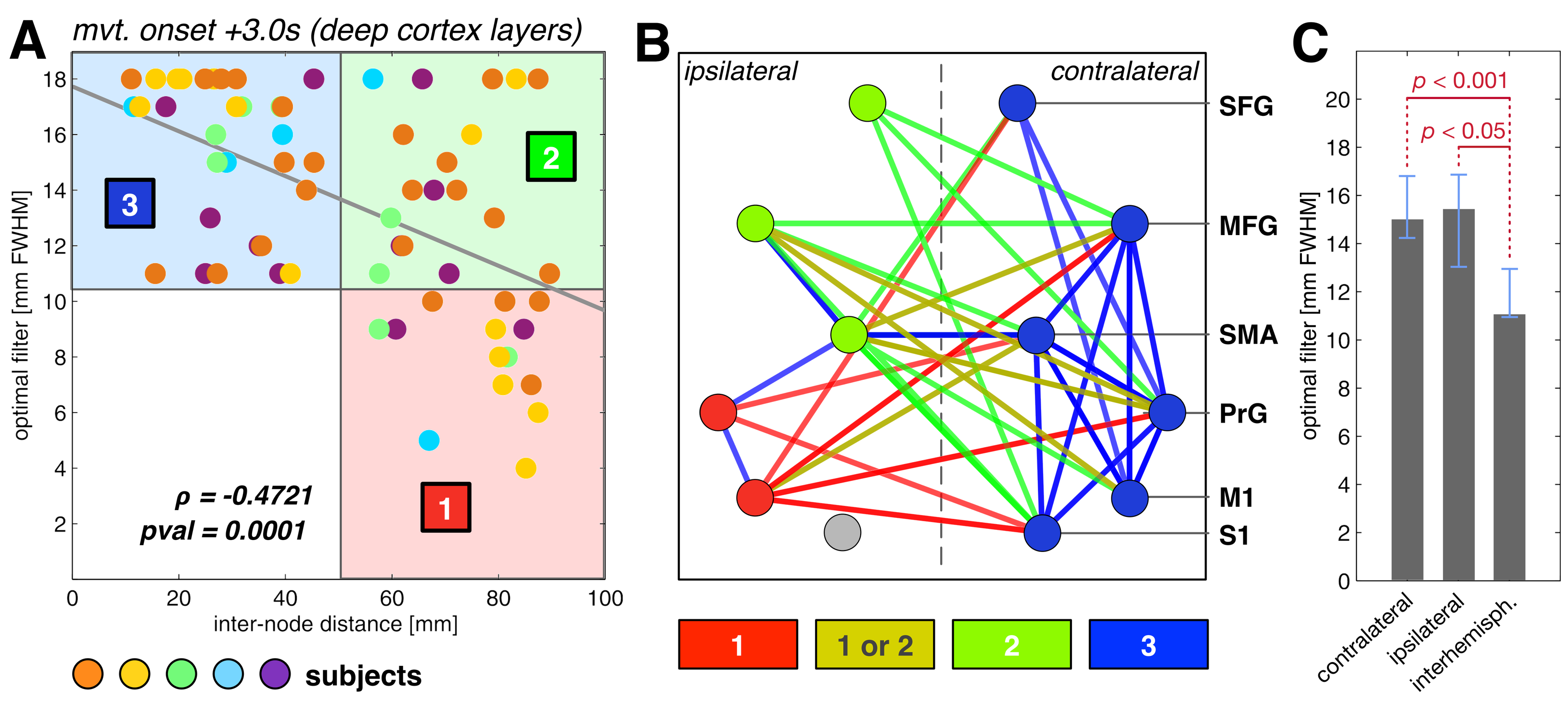

Figure 3: Optimal-filter network analysis. Distances between regional nodes were estimated and their relationship to optimal filter width was established for each connection; Spearman's *rho* was used to measure correlation. **A)** We found robust distance-to-filter correlation in deep layers for the late time bin (*rho* = –0.4721; p = 0.0001). The results could be split into three groups (labelled 1 to 3) and traced back to the connection pattern shown in plot **B)**: nodes are colour-coded according to their dominant edge-group. **C)** Wilcoxon rank-sum test comparing median optimal filter width of contralateral, ipsilateral and inter-hemispheric connections.

Correspondence: roland.berkemeier@uniklinik-freiburg.de **Web:** www.ieeg.uni-freiburg.de

This work was (partly) supported by BrainLinks-BrainTools Cluster of Excellence funded by the German Research Foundation (DFG, grant number EXC 1086)